ELECTROKINETICS OF A FLUID-SATURATED ROCK SAMPLE: LABORATORY EXPERIMENTS

by

Zhenya Zhu and M.N. Toksöz

Earth Resources Laboratory
Department of Earth, Atmospheric, and Planetary Sciences
Massachusetts Institute of Technology
Cambridge, MA 02139

ABSTRACT

The conversion between seismic and electromagnetic energies was discovered in a fluid-filled porous formation. When seismic waves propagate through a fluid-saturated porous formation, relative motion between the pore fluid and the solid matrix is generated and cation motion in the fluid is formed. The streaming electric current induces electromagnetic waves in the formation. There is an opposite phenomenon, i.e., the conversion of electric energy into acoustic energy in the porous formation. The electroseismics in porous sandstone samples are investigated by ultrasonic experiments in our laboratory. A compressional or a shear transducer excites an acoustic wave in the water-saturated sample and the electric signals generated on the surface are measured by an electrode. The relationship between the electric potential and acoustic wave or the conductivity of water-saturated rocks is studied. The electro-seismic conversion in rock samples is also investigated. Electroseismics could provide an effective means for estimating the fluid-saturated porous formation.

INTRODUCTION

Electrokinetics is the coupling and conversion between seismic and electromagnetic energies. The electrokinetic phenomena were discovered and proposed to be used as an exploration tool in the thirties (Thompson, 1936; Belluigi, 1937). When a seismic wave propagates in a fluid-filled porous formation, it generates vibration of the rock grains and pore fluid and a relative displacement between them. The relative motion distorts the electric balance of the surface dipoles and produces an electromagnetic wave. On the other hand, when the pore fluid with cations has a relative motion enforced by an electric field, the relative action between the grain and the pore fluid generates seismic wave.

Many laboratory experiments (Broz and Epstein, 1976; Ishido and Mizutani, 1981; Kuin and Stein, 1987; Cerda and Kiry, 1989; and Morgan et al., 1989) were performed to investigate the streaming potentials generated by the flowing of different fluids at different pressures through porous sands or man-made porous material. Theoretical studies demonstrated the electrokinetic effects in porous media (Kozak and Davis, 1987;

Neev and Yeatts, 1989; Thompson and Gist, 1991; Pride et al., 1991, 1993). The electroseismic effects were also observed in the field testing (Martner and Sparks, 1959; Sobolev et al., 1984; Russell and Barker, 1991; Thompson and Gist, 1993).

We investigate the electrokinetics of a fluid-saturated sandstone in our ultrasonic laboratory. The electromagnetic signals generated by acoustic waves with different modes and the acoustic waves generated by an electric pulse in the water-saturated sandstone samples are observed and measured. The relationship between the acoustic amplitude and the electric potential, and the effect of the fluid conductivity on the generated electromagnetic waves are investigated. The potentials measured on the surface of the fluid-saturated samples are compared with the dry sandstone samples and some dry insulators. The electro-seismic conversion in the fluid-saturated samples is also investigated.

EXPERIMENTS OF SEISMO-ELECTRIC CONVERSION

Some experiments which demonstrate the seismo-electric conversion are performed with the rock samples. The main properties of electrokinetics in a fluid-filled sandstone are investigated by the experiments.

Experiments with a Cylindrical Model

To study the seismo-electric conversion in a fluid-saturated porous material, the cylindrical samples are made of sandstone with different porosity, and the electric fields generated by different acoustic waves are measured by an electrode on the sample surfaces.

The samples made of Berea sandstone and Coconino sandstone are 1.24 cm in diameter and 10.0 cm in length. The density and the porosity of the Berea and Coconino samples are $2.08 g/cm^3$, 18.9% and $2.29 g/cm^3$, 13.2%, respectively.

A diagram of the experimental setup is shown in Figure 1. A water-saturated sample is placed between the acoustic source and receiver transducers. The constant coupling condition is kept during the experiment. The measurement points of 0.2 cm diameter are made of conducting glue on the sample surface along its axis. The spacing of the points is 1 cm. An electrode with a sharp pin-head touches these points and receives the electric potential on the surface. Received electric signals are amplified and filtered, then they are recorded. The whole sample is shielded by a metal film to prevent the outside electric influence.

Three acoustic modes, extensional, flexural and torsional modes, can be generated in a cylinder with a small diameter. In our experiments (Figure 1), if the source is a compressional wave transducer, an extensional wave can be generated in the cylinder sample; if it is a shear transducer, a flexural wave can be generated. To determine the acoustic mode, a small standard plane compressional transducer is applied to measure the acoustic wave on the circumference of the cylinder. When an extensional wave

propagates along the cylinder, the waveforms on the same circumference are the same, because they are axi-symmetric. When a flexural wave propagates along the cylinder, the received waveforms on the same circumference have opposite phase and different amplitude. If a torsional wave is generated in a cylinder, it cannot be received by a compressional wave.

The electric pulse exciting an acoustic transducer is a square pulse with high voltage of around 500 volts. The width of the pulse is variable and it is usually equal to the half cycle of the acoustic wave. The following results show the electric signals generated by extensional or flexural waves are received by an electrode on the sample surface.

Electric Signals Generated by an Extensional Wave

An extensional wave is generated by the compressional source transducer on the bottom end of the Berea sandstone sample shown in Figure 1. The alternate potential is measured by a sharp pin-electrode on the cylinder surface along its axis, and the electric signals are recorded in Figure 2.

The top trace in Figure 2 is the acoustic wave received by the compressional receiver on the other end of the cylinder sample. The center frequency of these waveforms is 18 kHz. The phase velocity determined by the slope of the waveforms is 1700 m/s.

From the time delay of the arrivals of the signals, we know that the signals are not an electric interference. If it were an electric interference, there would be no time delay in the arrivals. Comparing with the acoustic waveforms received on the other end of the samples, we can see that the shape and the arrival time of the acoustic waves coincide with those of the electric signals. This means that the electric signals are generated by the extensional wave propagating along the cylinder samples.

Electric signals generated by a flexural wave

Flexural waves can be generated by a shear source transducer shown in Figure 1. The electric signals received by an electrode on the surface of the Coconino cylinder sample are shown in Figure 3. The center frequency and the phase velocity of the signals recorded in Figure 3 are 27kHz and 1150 m/s, respectively. The particle motions of the extensional and flexural waves are different from each other. Once the relative motion between the pore fluid and the solid matrix is excited, the electromagnetic wave will be generated by the motion.

Experiments with Layer Models

One- or multi-layer models are made of water-saturated sandstone plates. The acoustic source is a compressional transducer fixed at the bottom of the plate. It generates a compressional wave and Rayleigh wave on the plate surface. The electric signals and acoustic waves are measured by an electrode and a small transducer, respectively.

One-layer Model

The one-layer model is shown in Figure 4. A compressional transducer as a source is located at the bottom of a water-saturated Berea sandstone plate whose thickness is 2.54 cm. Both the acoustic wave and the electric signal can be measured on the top surface by a compressional transducer and an electrode, respectively.

Figure 5 shows the acoustic waveforms (dashed lines) and the electric signals (solid lines). Comparing their shapes and arrival times, we can see they are very similar. The acoustic wave generates the electric signals. The main electric field is generated by the low-frequency Rayleigh wave, and those generated by the P-wave are very weak.

Multi-layer Model

A multi-layered model is shown in Figure 6. A water layer or a clay layer is sandwiched between the water-saturated Berea and Silver sandstone blocks, which are 2.54 cm in thickness and 15.24 cm by 12.54 cm on the sides. When the mid-layer is a 1 mm water-layer or 5 mm clay-layer, the electric signals on the top surface of the Silver block are received by an electrode and shown in Figure 7 and Figure 8, respectively. To compare their arrival time and the shapes of the waveforms, the electric signals received on the top surface of the Berea block are also plotted in dashed lines.

In the water case (Figure 7), the two sets of electric signals received on the tops of the Berea (dashed lines) and the Silver (solid lines) blocks almost have the same shapes and arrival times. The electric signals are generated at the interface of the Berea block and the water layer, then they, as an electromagnetic wave, propagate though the Silver block.

In the clay case (Figure 8), the electric signals received on the top of the Silver sample almost have the same shape and arrival time, but they are different from those on the top of the Berea sample. The electric signals generated at the interface of the Berea block and the clay form one electric signal due to the low conductivity of the clay layer, and it, as an electromagnetic signal passes through the top layer.

Relationship between the Acoustic and Electric Amplitudes

An electrode is fixed on a certain point of the sample shown in Figure 1 to receive the electric signal. The amplitude of the pulse exciting the P-wave source is increased step by step; the maximum electric amplitudes received by the electrode are recorded. Figure 9 shows the relationship between the electric signal and the voltage of the pulse exciting the transducer. This means that the amplitude of the electric signal is directly proportional to that of the exciting acoustic wave.

Effect of Fluid Conductivity

To study the effect of the saturant conductivity on the electrokinetics, we have measured the electric signals generated by the extensional wave in the Berea and Coconino sandstone samples which are saturated by water with different conductivity.

The sandstone samples are saturated in a vacuum system. The two bases of the cylinder samples are covered by the contacting glue. The resistance r of the cylinder along its axis can be measured with a multimeter. The resistivity R is calculated as

$$R = r\frac{A}{L} \tag{1}$$

where A and L are the sectional area and the length of the cylinder sample. The resistivity of the samples can be changed by immersing the samples into the saturants with different conductivity, which are pure water or brine with different salt concentration. After the samples are immersed in the saturants for at least eight hours, the resistivity becomes very stable.

Figure 10 shows the relationship between the resistivity of the saturated samples and the average amplitude of the generated electric signals in the Berea and Coconino cylinder samples (Figure 1). It shows the effect of the electric concentration of the pore fluid on the electrokinetics. The larger the resistivity of the sample, the larger is the amplitude of the generated signal.

If the sample is saturated by an insulator fluid, such as alcohol, the resistivity will be infinite. In this case, no electric signal can be generated, because there is no any cation or anion in the saturant.

The experiments show that the electroseismics are related to the relative motion of the cation in the fluid.

Experiments with Dry Samples

The previous experiments show the effect of the pore fluid on the electrokinetics. To understand this effect, the same measurements as shown in Figure 1 are performed with the dry cylinder sandstone sample and some dry insulator samples, such as plastics, wood and glass cylinders. Very weak electric signals can be generated by the acoustic wave on these dry samples. The amplitudes on the insulators are about $5\mu V$, comparing that in Figure 10. Figure 11 shows the electric signals on a dry Berea sandstone sample. The maximum amplitude of the signals is around $20\mu V$. From Figure 11, we can see that not only the amplitudes but also the phases of the first arrivals are different from each other. They are generated by an acoustic wave and due to either the piezoelectric effect of the quartz grains in the sandstone samples or vibration of the electric charges on the insulator surface. The mechanism is different from that of the electrokinetics in the fluid-saturated porous medium.

EXPERIMENTS OF ELECTRO-SEISMIC CONVERSION

In the previous experiments, the acoustic transducer excites the electromagnetic wave on the surface. The acoustic energy converts into electric energy. In the following experiments, we have studied the opposite energy conversion from electric energy into acoustic energy. An electric pulse with high voltage is connected with the electrodes on the sample and the electric field is excited by it. The alternate electric field generates an acoustic wave which can be received by a transducer. The extensional and flexural waves are generated by ring electrodes and parallel electrodes in the water-saturated Berea sandstone samples.

Figure 12 shows the schematic diagram of the experimental setup with the ring electrodes. The ring electrodes are made on the top end of the sample. An electric pulse with high voltage (around 400 V) is step by step connected to the electrodes. Acoustic waves can be received by a compressional transducer on the other end of the sample (Figure 13). From the arrival times of the received acoustic waves, we know that the extensional waves are generated by the electric pulse at the different regions of the sample.

The frequency of the acoustic waves is almost the same because of the same distance of the excited regions. If the spacing of the electrodes is changed, the frequency of the acoustic waves will be changed. The shorter the spacing, the higher is the frequency. If the phase of the electric pulse is changed, the phase of the acoustic wave will be opposite.

Figure 14 shows a schematic diagram of parallel electrodes. Two electrodes are made on the end of the square cylindric sample. The acoustic wave generated by the electric pulse can be received by a shear transducer which is located on the other end of the sample. When the polarization of the shear transducer is located at the positions of 1#(0^o), 2#(90^o), and 3#(180^o), respectively, the received waveforms are shown in Figure 15.

To study the phase characteristic of the acoustic wave, the interference signals excited by the pulse is maintained in the record. The arrival times and the phases are the same for electric interference, but the phase of the acoustic waves which arrive later varies with the polarization of the shear transducer. The direction of the particle motion of the wave is the same as that of the electric field. This shows a flexural wave propagating along the cylindric sample.

If the above experiments are repeated with a dry sandstone sample, no acoustic wave can be received. This means that the relative motion between the solid matrix and the cation in the pore fluid generates the acoustic waves. This principle is completely different from piezoelectrics.

CONCLUSIONS

The electrokinetics in a fluid-saturated porous sandstone and the conversion between acoustic and electric energies are demonstrated in our experiments. The electromagnetic wave can be generated by the acoustic wave with different modes; the acoustic wave also can be generated by the alternate electric fields.

The frequency of the electromagnetic wave generated in seismo-electric conversion is related to the center frequency of the acoustic wave; its amplitude is directly proportional to that of the acoustic wave. The frequency of the acoustic wave generated in electro-seismic conversion is related to the region excited by the electric field. When the conductivity of the pore fluid decreases, the amplitude of the generated electromagnetic wave increases. But if the pore fluid is an insulator, no electromagnetic wave can be generated. Electrokinetics would be a very useful means for exploring the porous formation.

ACKNOWLEDGEMENTS

We would like to thank Dr. A.H. Thompson of Exxon, Dr. S. Pride, Prof. T.R. Madden and Mr. F. Guler for their valuable suggestions and useful discussions. This study is supported by the Borehole Acoustics and Logging Consortium at M.I.T., and Department of Energy grant DE-FG02-93ER14322.

REFERENCES

Belluigi, A., 1937, Seismic-electric prospecting, *The Oil Weekly,* 38–42.

Broz, Z., and N. Epstein, 1976, Electrokinetic flow through porous media composed of fine cylindrical capillaries, *J. Colloid and Interface Science, 56,* 605–612.

Cerda, C.M., and Non-Chhom Kiry, 1989, The use of sinusoidal streaming flow measurements to determine the electrokinetic properties of porous media, *Colloids and Surfaces, 35,* 7–15.

Ishido, T., and H. Mizutani, 1981, Experimental and theoretical basis of electrokinetic phenomena in rock-water system and its applications to geophysics, *J. Geophys. Res., 86,* 1763–1775.

Kozak, M.W., and E.J. Davis, 1989, Electrokinetics of concentrated suspensions and porous media, *J. Colloid and Interface Science, 127,* 497–510.

Kuin, A.J., and H.N. Stein, 1987, Development of a new pore model: II Electrokinetic transport properties, surface conductance, and convective charge transport, *J. Col-*

loid and Interface Science, 115,188–198.

Martner, S.T., and N.R. Sparks, 1959, The electroseismic effect, *Geophysics, 24,* 297–308.

Morgan, F.D., E.R. Williams, and T.R. Madden, 1989, Streaming potential properties of westerly granite with applications, *J. geophys. Res., 94,* 12449–12461.

Neev, J., and F.R. Yeatts, 1989, Electrokinetic effects in fluid-saturated poroelastic media, *Physical Review B, 40,* 9135–9142.

Pride, S.R., and F.D. Morgan, 1991, Electrokinetic dissipation induced by seismic wave, *Geophysics, 56,* 914–925.

Pride, S.R., F.D. Morgan, and A.F. Gangi, 1993, Drag force of porous-medium acoustics, *Physical Review B, 47,* 4964–4978.

Russell, R.D., and A.S. Barker, Jr., 1991, Seismo-electric exploration: Expected signal amplitudes, *Geophys. Prosp., 39,* 105–118.

Sobolev, G.A., V.M. Demin, B.B. Narod, and P. Whaite, 1984, Tests of piezo-electric and pulsed-radio methods for quartz vein and base-metal sulfides prospecting at Giant Yellowknife Mine, N.W.T., and Sullivan Mine, Kimberley, Canada, *Geophysics, 49,* 2178–2185.

Thompson, A.H., and G.A. Gist, 1991, Electroseismic pros- pecting, *SEG 61st Annual Meeting, Paper EM2.1,* 425–427.

Thompson, A.H., and G.A. Gist, 1993 Geophysical applications of electrokinetic conversion, *The Leading Edge, 12,* 1169–1173.

Thompson, R.R., 1936, The seismic electric effect, *Geophysics, 1,* 327–335.

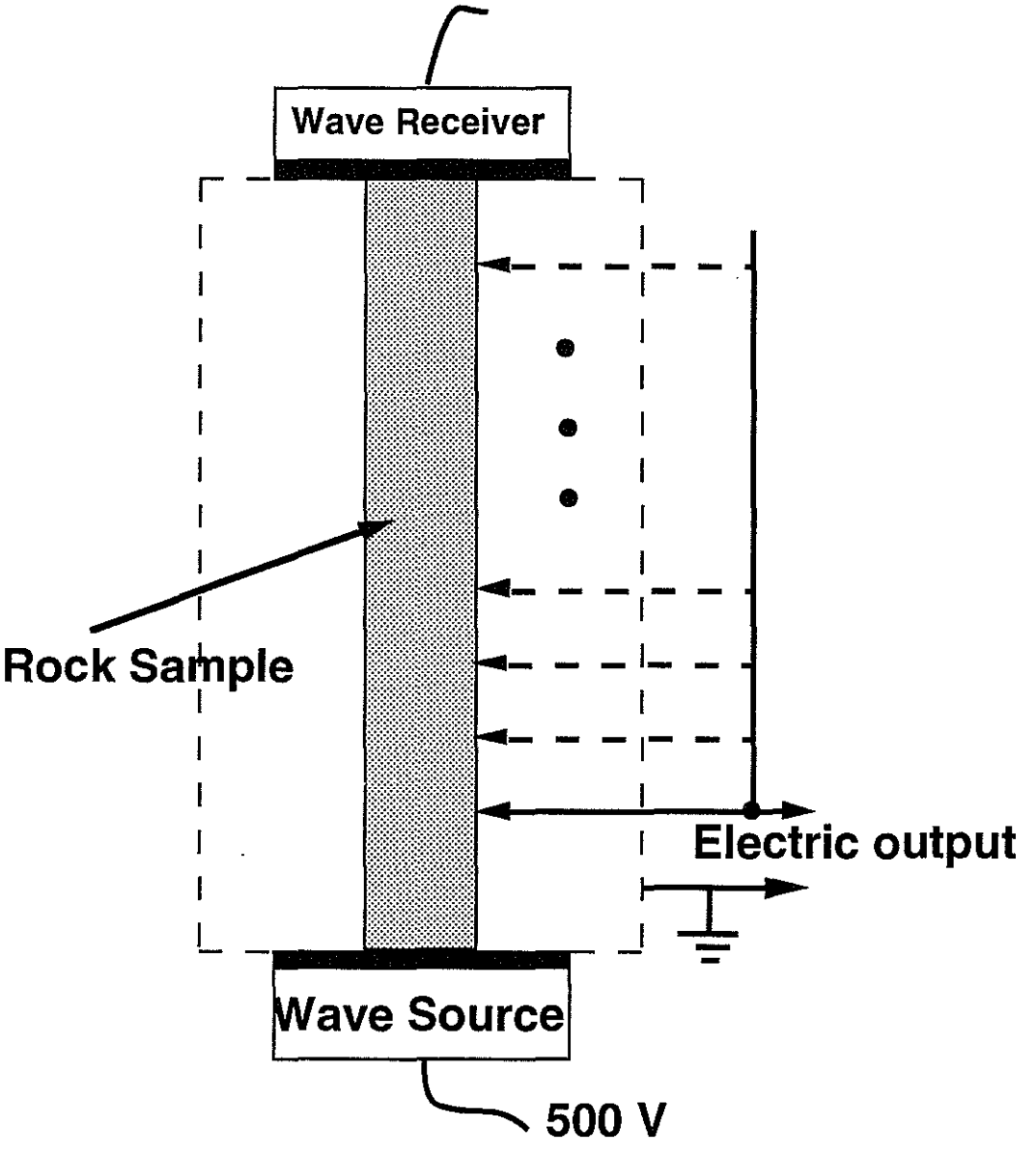

Figure 1: A diagram for measuring the electric field generated by a transducer in a fluid-saturated rock sample. The sample is a cylinder with 10 cm in length and 1.25 cm in diameter.

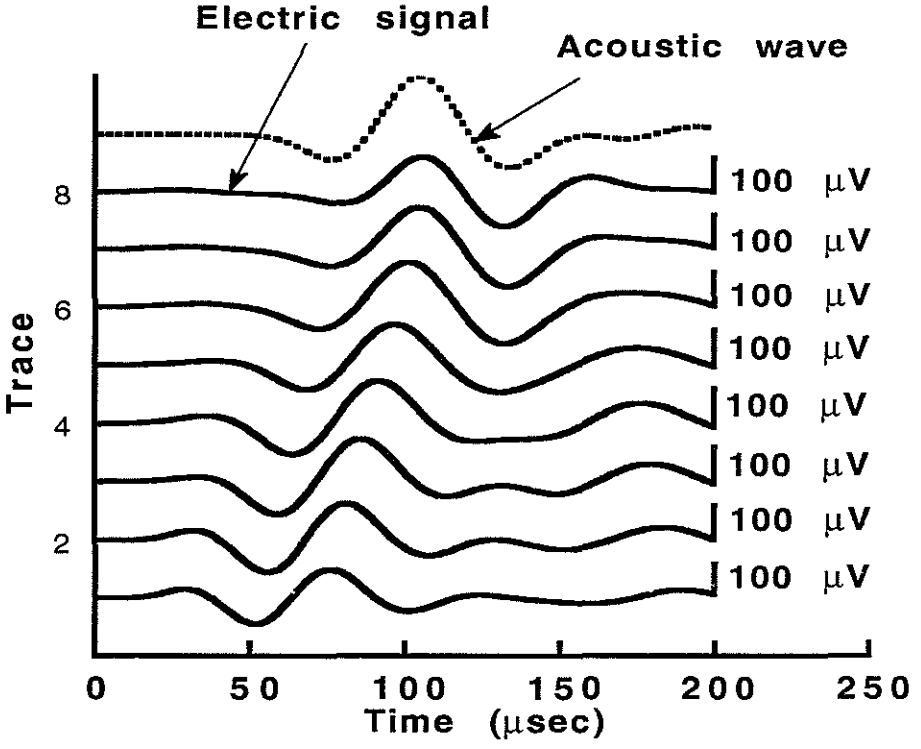

Figure 2: Electric waveforms generated by a P-wave transducer in the water-saturated Berea sandstone sample. The top trace (dashed line) are the seismic waveform received by the transducer at the other end of the sample.

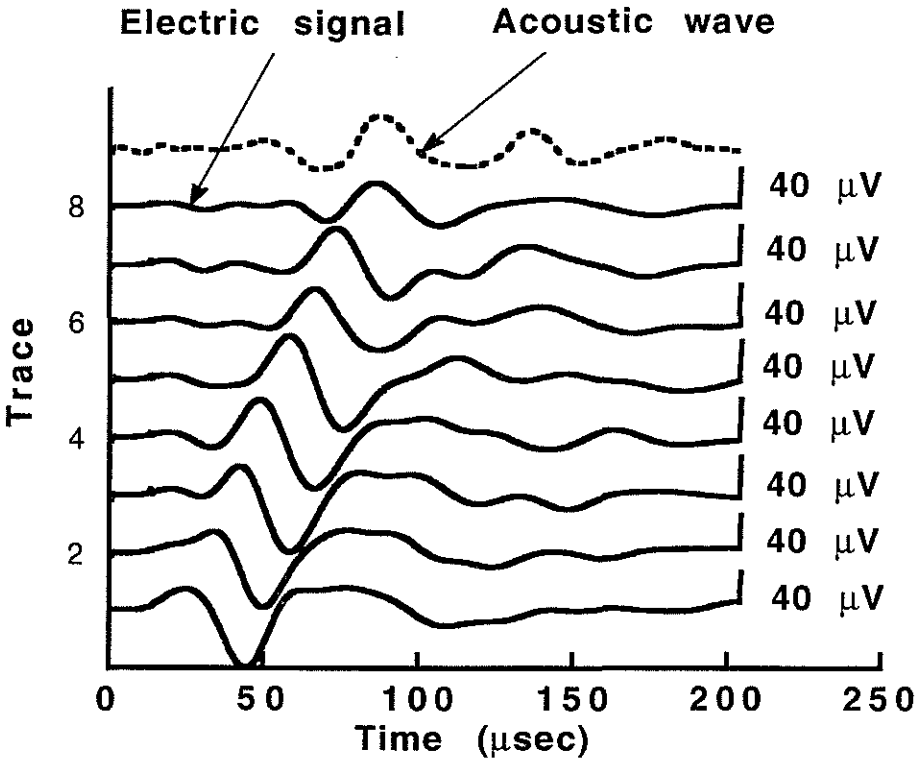

Figure 3: Electric waveforms generated by an S-wave transducer in the water-saturated Coconino sandstone sample. The top trace (dashed line) is the seismic waveform received by the transducer at the other end of the sample.

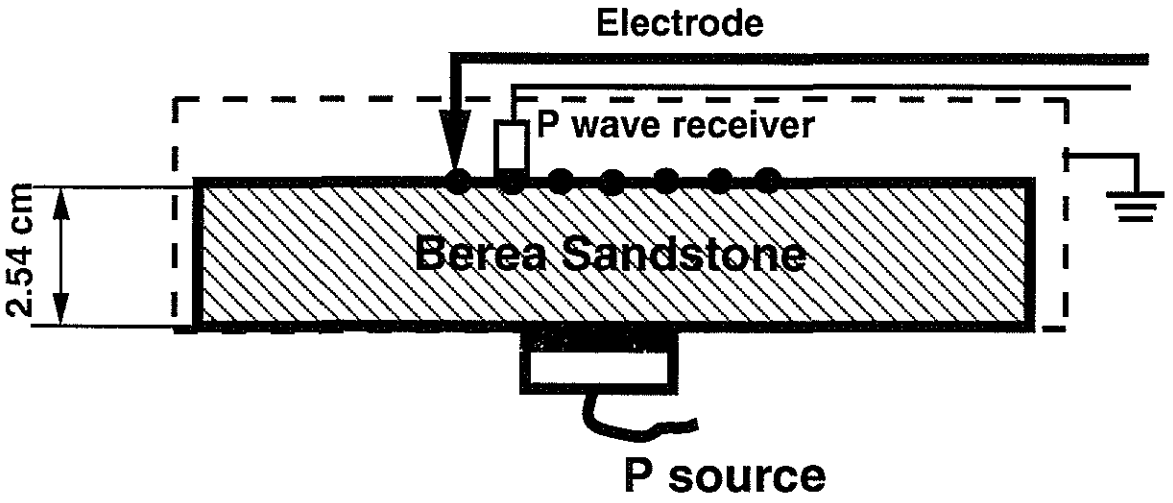

Figure 4: A diagram of a one-layer model.

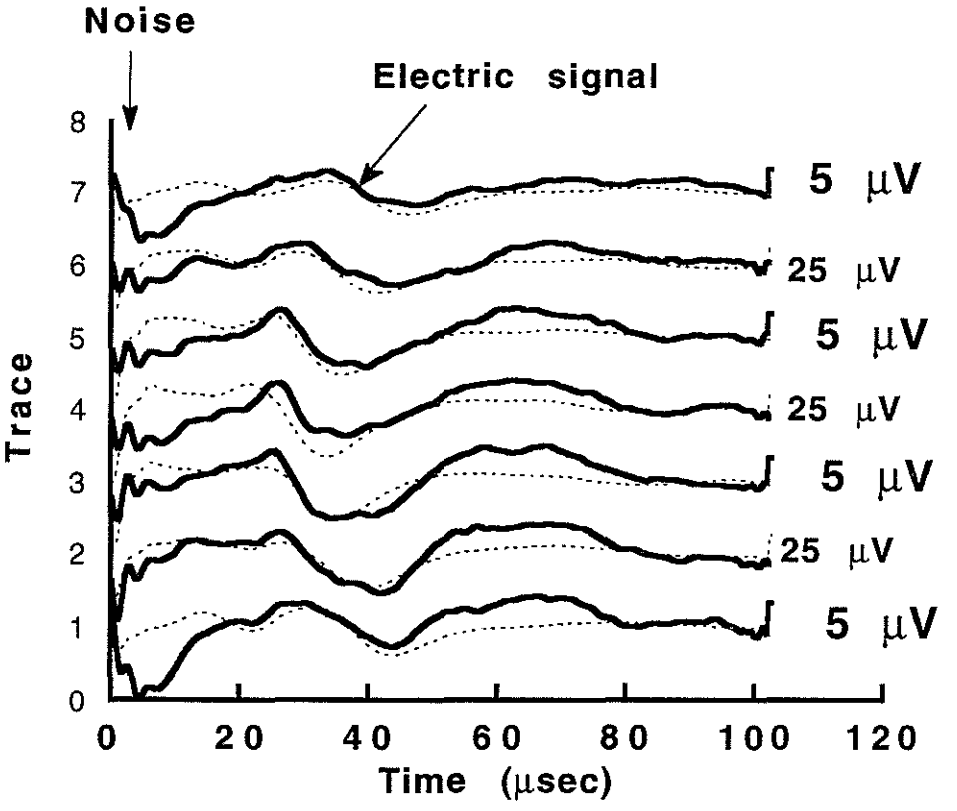

Figure 5: The seismic waveforms (dashed lines) as well as electric signals (solid lines) generated by a P- wave source in the one-layer model.

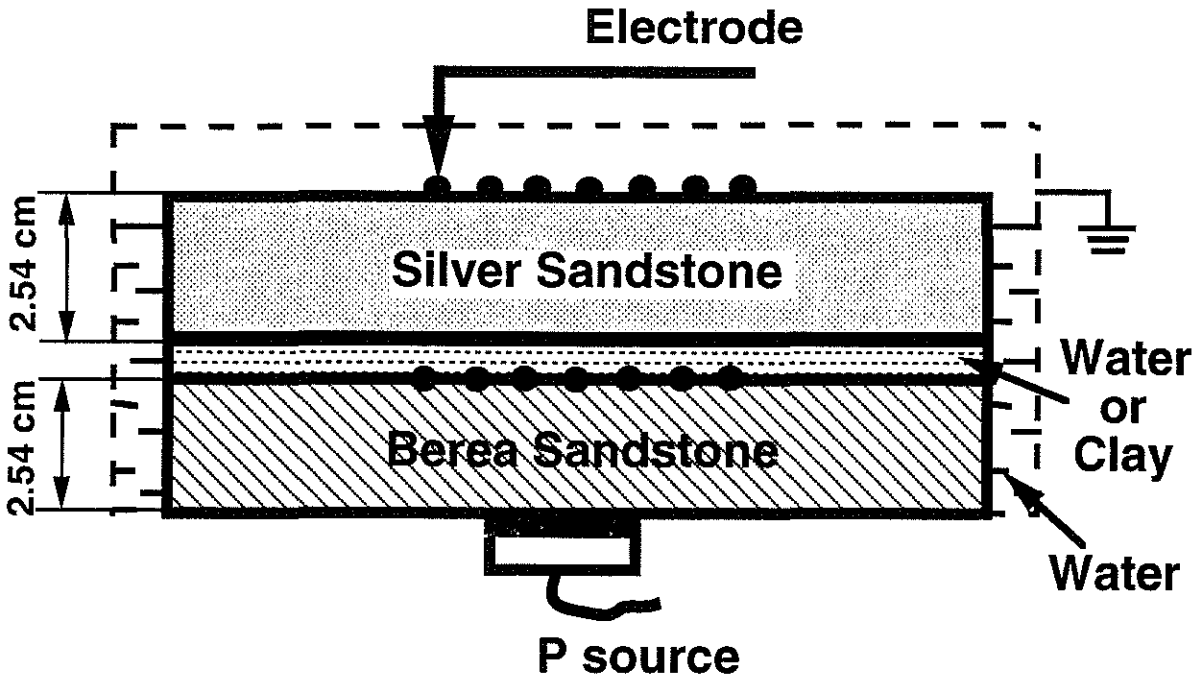

Figure 6: A diagram of a Multi-layer model.

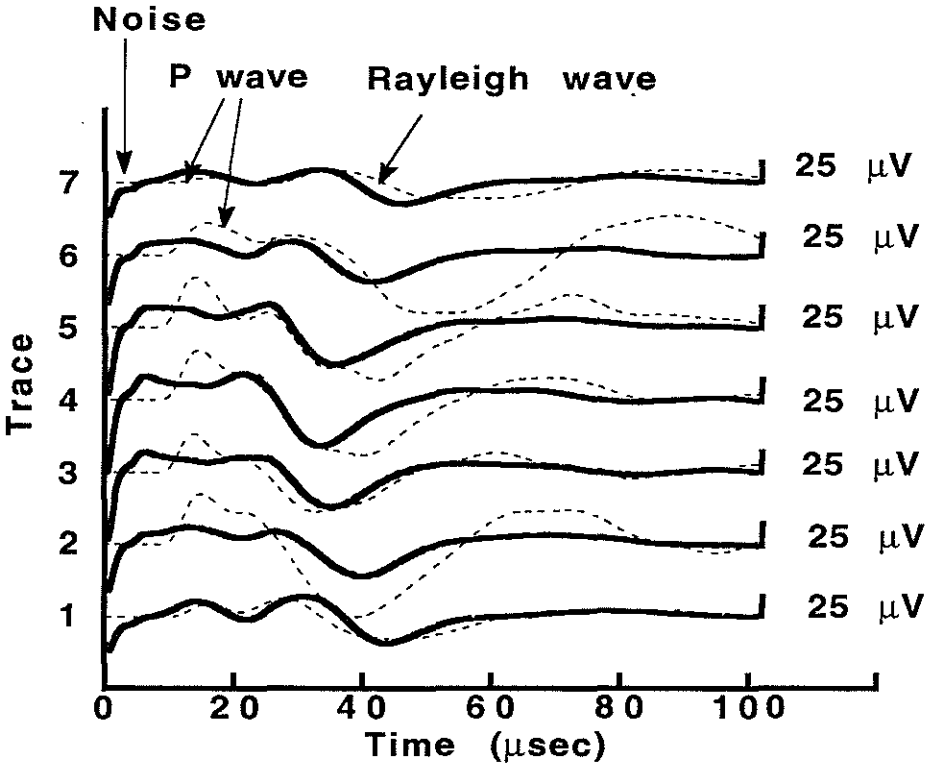

Figure 7: Electric waveforms (solid lines) received on the top surface of the Silver sandstone block in the water-layer model. The thickness of the water is 1 mm. The dash lines show the electric signals received on the top surface of the Berea sandstone block.

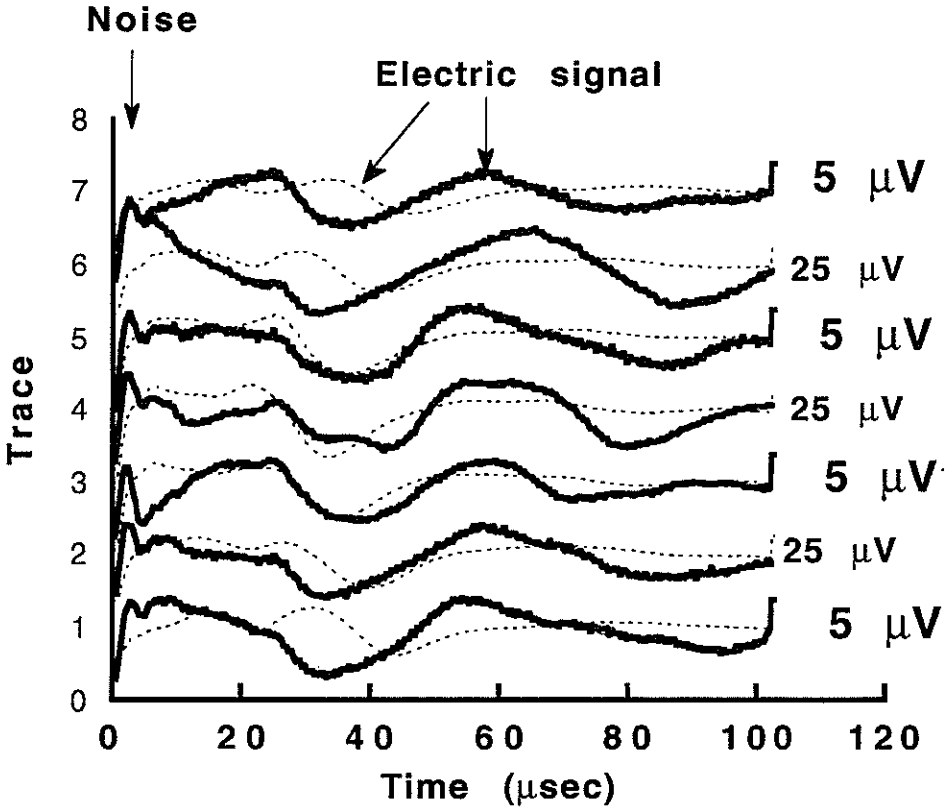

Figure 8: Electric waveforms (solid lines) received on the top surface of the Silver sandstone block in the clay-layer model. The thickness of the clay is 5 mm. The dashed lines show the electric signals received on the top surface of the Berea sandstone block.

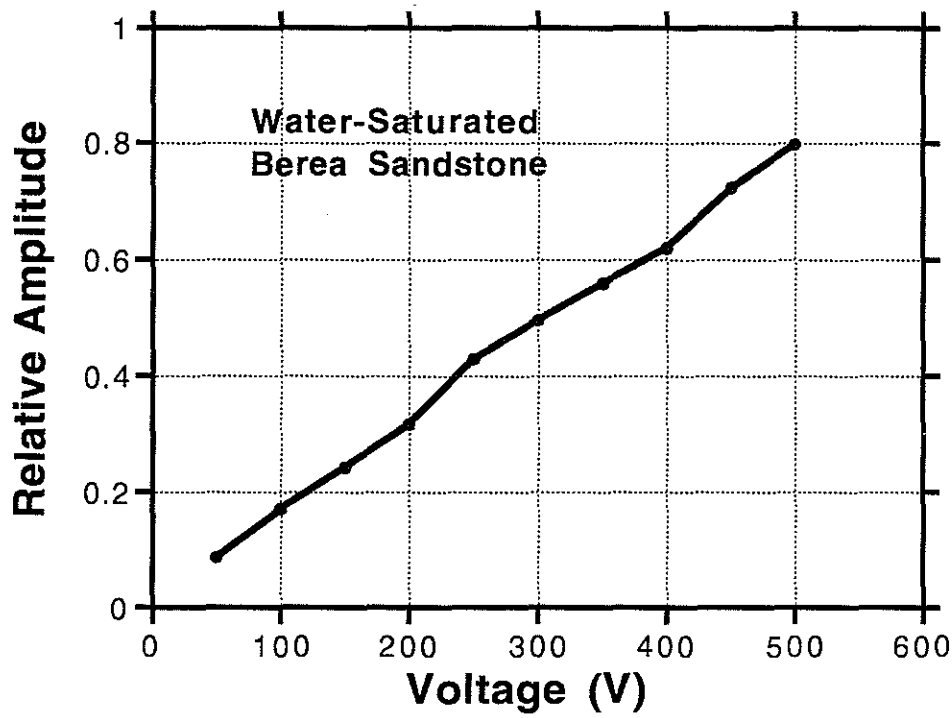

Figure 9: Relationship of the electric amplitude and the voltage generated by the acoustic wave in the water-saturated Berea sample.

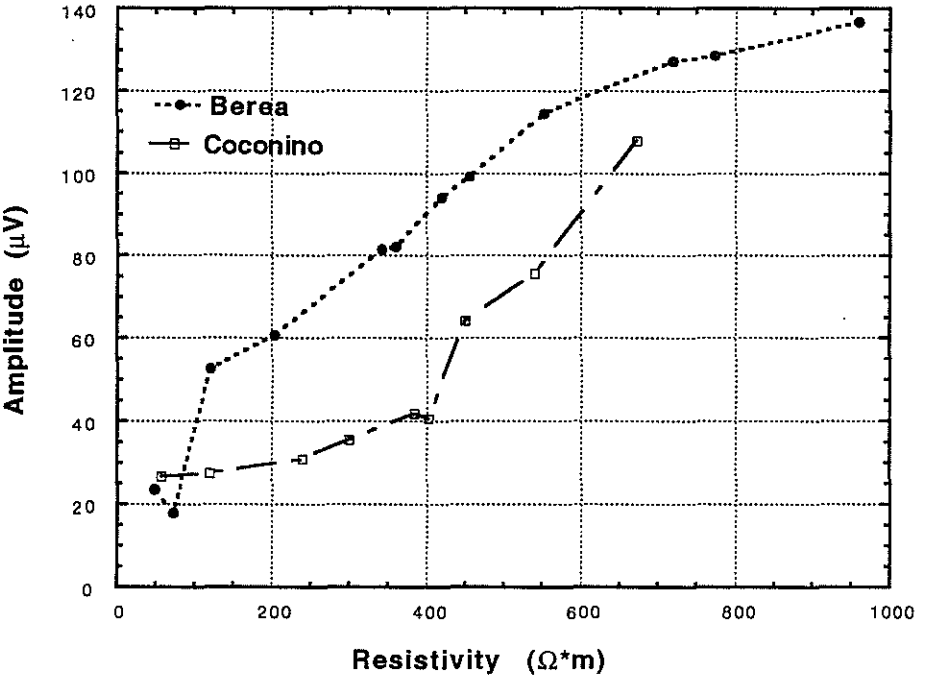

Figure 10: Relationship of the electric amplitude and the resistivity of the water-saturated samples.

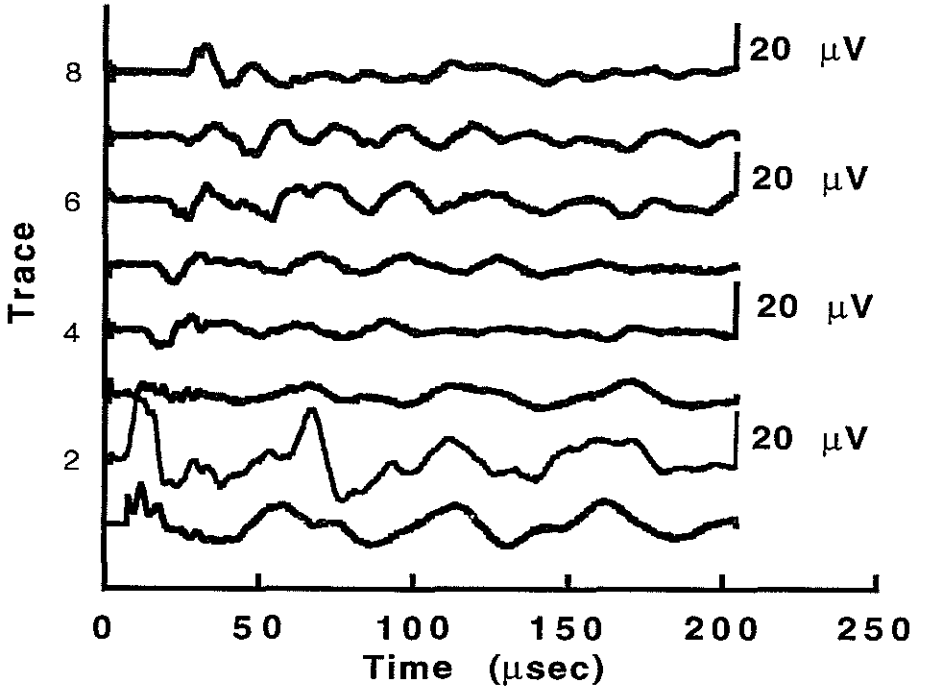

Figure 11: Electric signals received on the dry Berea sandstone sample. The phases of the first arrivals are different from each other.

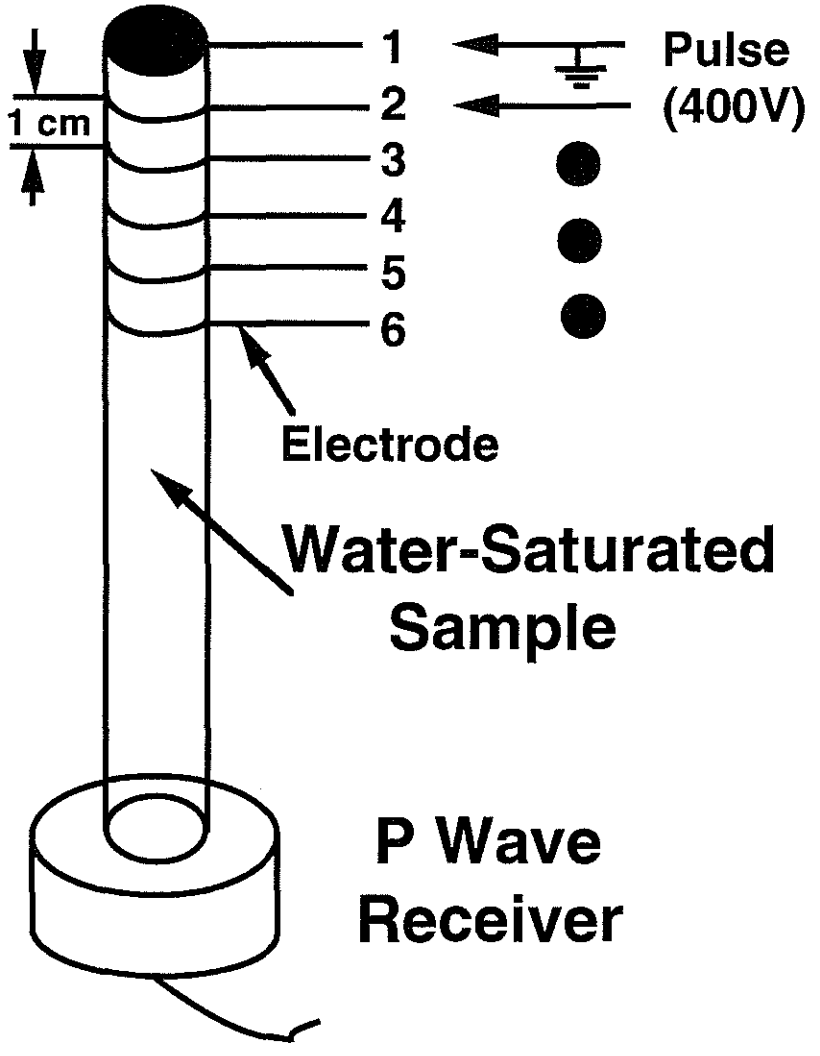

Figure 12: A diagram measuring the seismic wave generated by the electric pulse with ring electrodes.

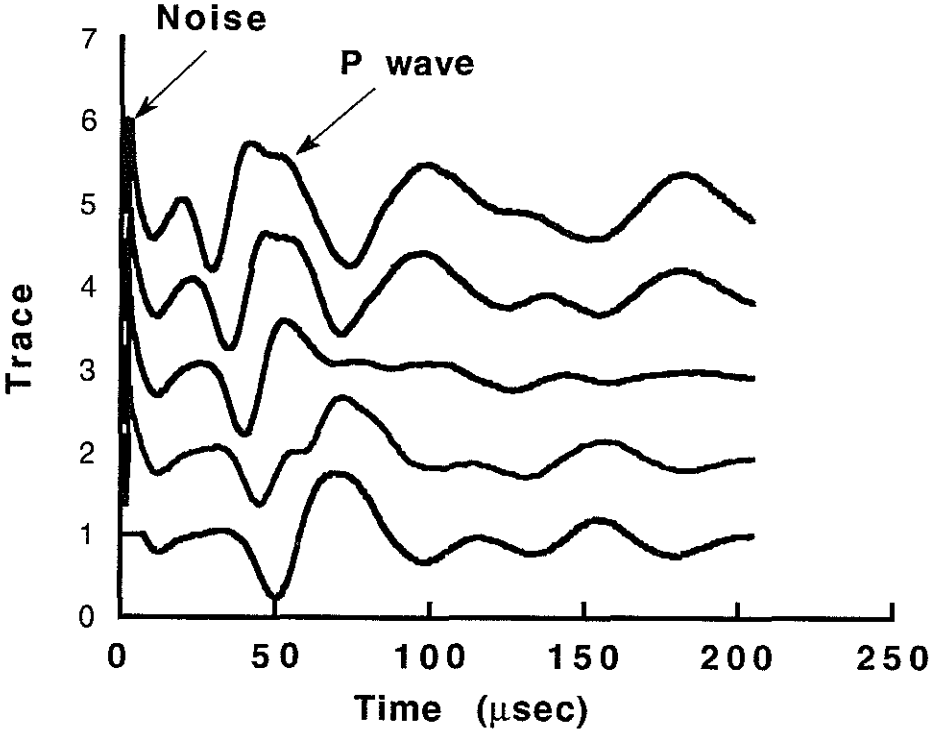

Figure 13: The acoustic waveforms received by the P-wave transducer in the experiments shown in Figure 12.

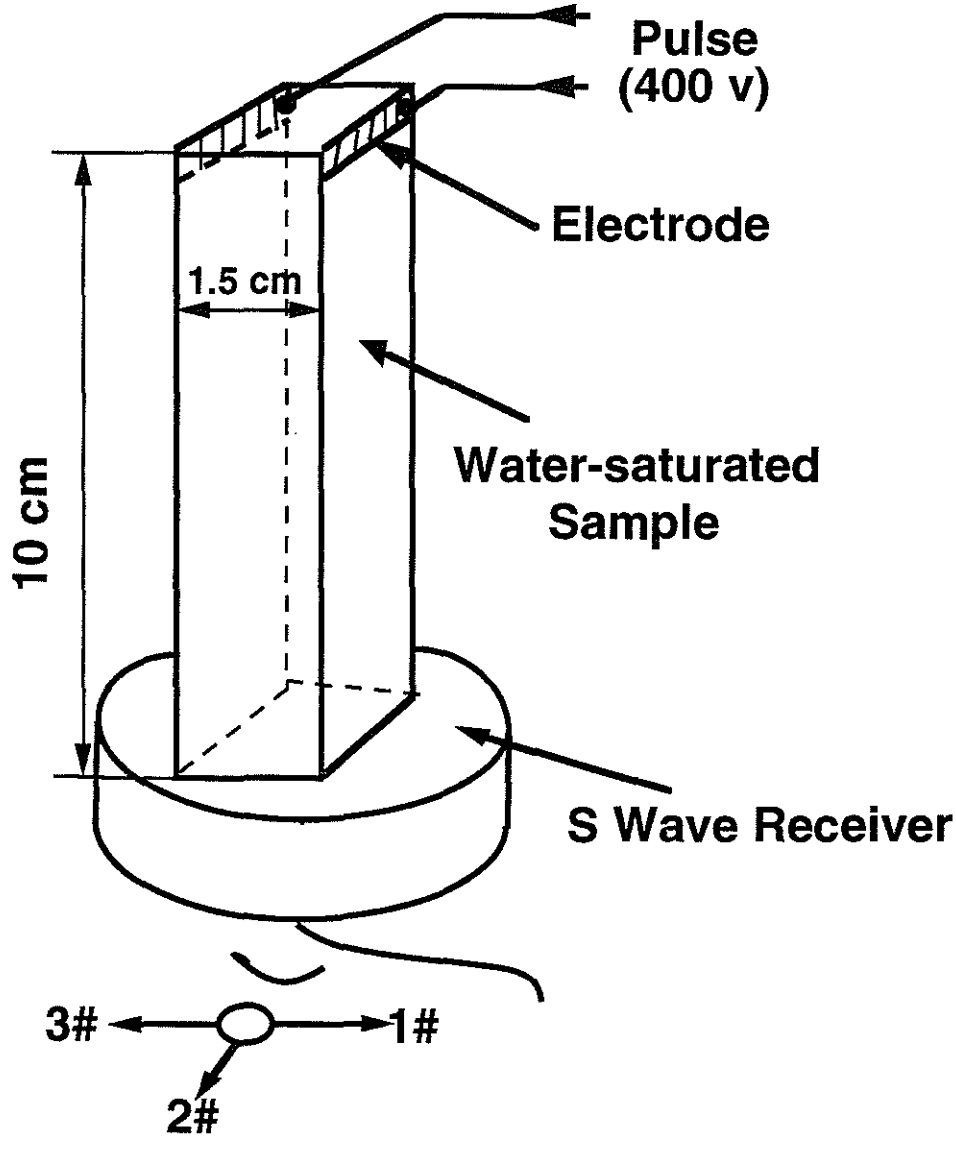

Figure 14: A diagram measuring the seismic wave generated by the electric pulse with the parallel electrodes.

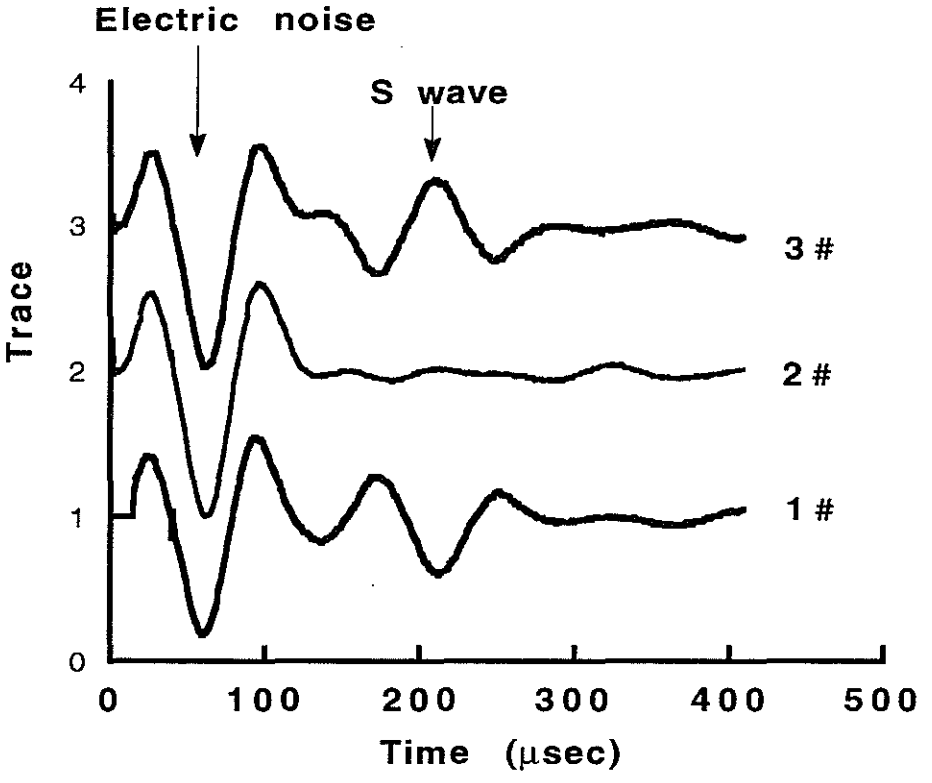

Figure 15: The seismic waveforms received by the S-wave transducer at positions 1#, 2#, and 3#.